

See discussions, stats, and author profiles for this publication at: <https://www.researchgate.net/publication/273518851>

A Quasiclassical Trajectory Study of the Reaction of H Atoms with O₂ ($1 \Delta g$)

ARTICLE *in* THE JOURNAL OF PHYSICAL CHEMISTRY A · FEBRUARY 2015

Impact Factor: 2.69 · DOI: 10.1021/jp510202r

CITATION

1

READS

41

2 AUTHORS, INCLUDING:



Péter Szabó

University of Pannonia, Veszprém

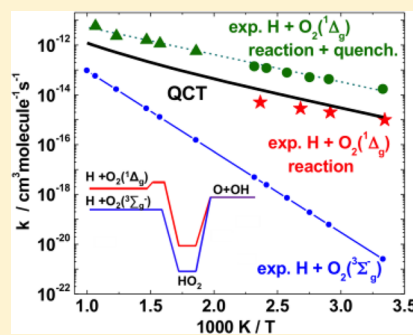
3 PUBLICATIONS 2 CITATIONS

SEE PROFILE

A Quasiclassical Trajectory Study of the Reaction of H Atoms with $O_2(^1\Delta_g)$ Péter Szabó[†] and György Lendvay^{*,†,‡}[†]Department of General and Inorganic Chemistry, Institute of Chemistry, University of Pannonia, P.O.B. 158, Veszprém H-8201, Hungary[‡]Institute of Materials and Environmental Chemistry, Research Centre for Natural Sciences, Hungarian Academy of Sciences, Magyar Tudósok krt. 2., Budapest H-1117, Hungary

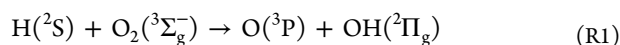
Supporting Information

ABSTRACT: The kinetic and dynamic characteristics of the reaction of H atoms with electronically excited O_2 were studied using the quasiclassical trajectory (QCT) method and the potential energy surface of Li et al. (*J. Chem. Phys.* **2010**, *133*, 144306–144314). The reaction takes place via a deep potential well that can be entered by climbing a barrier in the reactant valley and can be left without a barrier on the product side. In this reaction, the basic assumptions of statistical rate theories are not fulfilled: (i) 80% of the trajectories cross the barrier region twice and are nonreactive; (ii) the energy is not equilibrated in the HO_2 potential well. The QCT cross sections agree well with those from the existing exact quantum-mechanical data and extend them to vib-rotationally excited reactants. The thermal rate coefficients agree well with measurements of pure reactive quenching of $O_2(^1\Delta_g)$ and are lower than those involving both reactive and electronic quenching. The temperature dependence is described as $k_2 = 5.81 \times 10^{-16} T^{1.45} \exp(-2270/T) \text{ cm}^3 \text{ molecule}^{-1} \text{ s}^{-1}$. On the basis of a comparison of the QCT data with the two kinds of experiments, we estimate that electronic quenching is faster than reaction by a factor of about 10 at low and 2 at high flame temperatures.

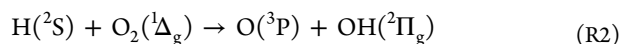


INTRODUCTION

The reaction of H atom with dioxygen has been termed “the single most important” elementary step in combustion.¹ Its importance comes from the fact that it is a chain-branching step, yielding two active species, O atom and OH radical, starting from one, the H atom. This is the step that introduces O_2 into the chain of reactions. At high pressures the HO_2 intermediate is collisionally stabilized, making the reaction a chain-termination step. Because of its importance, the reaction has been the subject of a large number of studies, both experimental and theoretical.^{2–27} A large body of information is available on the reaction of H atoms with oxygen molecules in the electronic ground state:



Both the kinetics and the dynamics of the reaction, including collisional energy transfer, are quite well established. Much less is known about the reaction of singlet molecular oxygen, $O_2(^1\Delta_g)$, with H atoms:



This reaction seems also to be feasible in the higher stratosphere and in high-temperature flames. Application of excitation of molecular oxygen to the singlet state was proposed decades ago as a way to accelerate combustion.²⁸ Electronically excited oxygen will not necessarily be present in flames even at

high temperatures, but it is produced in almost all oxygen-containing plasmas because the energy needed to excite $O_2(^3\Sigma_g^-)$ is relatively low (94.5 kJ/mol).²⁹ The radiative lifetime of $O_2(^1\Delta_g)$ is relatively long (>3800 s),³⁰ so it can live long enough in flames to perturb the kinetics of combustion if it proves to be reactive enough. It is known that the barrier on the potential energy surfaces of its reactions with closed-shell molecules is high, but it can easily react with open-shell reactants. Both the experiments in which the reaction mixture was directed to pass through an electric discharge and the related combustion modeling studies^{31–36} demonstrated that the concept works: the flame velocity was found to increase in the presence of electronically excited dioxygen.

Several experimental studies^{37–42} of the kinetics of the reaction of $O_2(^1\Delta_g)$ with hydrogen atoms have been reported. Early work^{37,38} resulted in estimates of the rate coefficient. Schmidt and Schiff³⁹ followed the $O_2(^1\Delta_g)$ concentration to get the rate of loss due to collisions with H atoms at room

Special Issue: 100 Years of Combustion Kinetics at Argonne: A Festschrift for Lawrence B. Harding, Joe V. Michael, and Albert F. Wagner

Received: October 9, 2014

Revised: January 14, 2015

Published: February 10, 2015

temperature and obtained a rate coefficient of $2.5 \times 10^{-14} \text{ cm}^3 \text{ molecule}^{-1} \text{ s}^{-1}$. The technique they used does not allow a distinction between chemical reaction and physical quenching. Cupitt et al.⁴⁰ measured the rate at several temperatures between 300 and 430 K and argued that chemical reaction dominates in the process. The Arrhenius parameters they derived are shown in Table 1. Basevich and Vedenev⁴¹ did

Table 1. Experimental Thermal Rate Coefficients for Reaction R2

reaction	A	E_a	T range	ref
	$\text{cm}^3 \text{ molecule}^{-1} \text{ s}^{-1}$	kJ/mol	K	
R2 with quenching	1.46×10^{-11}	16.75	300–423	40
R2 with quenching	1.82×10^{-10}	26.30	520–933	41
R2 with quenching	6.55×10^{-11}	21.03	300–933	31
R2	1.83×10^{-13}	13.00	299–423	42

similar experiments at higher temperatures (500–800 K). The corresponding Arrhenius parameters differ from those of Cupitt et al.,⁴⁰ the activation energy being more than 50% higher. Several years later, Popov³¹ combined the rate coefficients measured in the two studies and found the measured points to lie along essentially the same line in the Arrhenius representation. The Arrhenius parameters he derived (Table 1) have been widely used in flame simulations.

The latest reported experiments were performed by Hack and Kurzke,⁴² who showed that the rate of reaction R2, with or without physical quenching, cannot be determined if only the concentration of the reactants is monitored. They derived the rate coefficients of the pure chemical step R2 by following the concentrations of H and O atoms as well as OH radicals and fitting a complex model including about 20 reactions to the measured data. The values they obtained in the temperature range of 299–423 K are smaller by about an order of magnitude than those measured by Cupitt et al.,⁴⁰ indicating that the reactive rate is below 10% of the total rate of $\text{O}_2(^1\Delta_g)$ removal. It should be noted that under the conditions of the Hack and Kurzke experiment, the possible loss of $\text{O}_2(^1\Delta_g)$ is negligible because of the small initial H atom concentration, so physical quenching, if occurs, does not influence the radical concentration profiles.

Early theoretical studies were based on the assumption that the activation energy of the reaction of singlet molecular oxygen can be derived from that of the reaction of ground-state oxygen from a simple curve-crossing model.⁴³ This view seems to be oversimplified in light of the recent calculations of the potential energy surface (PES) of the reaction by Li et al.⁴⁴ using high-level electronic structure methods. Figure 1 shows

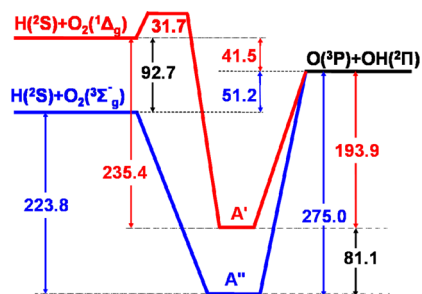


Figure 1. Energies (in kJ/mol) of the stationary points of the potential energy surfaces of reactions R1 (blue) and R2 (red).

the major features of the excited-state PES in comparison with those of the ground-state reaction. There is a deep potential well corresponding to HO_2 on both PESs. The two potential surfaces are degenerate on the product $\text{O} + \text{OH}$ side. However, there are some qualitative differences between the PESs for the two electronic states. The reaction of $\text{O}_2(^3\Sigma_g^-)$ is endothermic and displays no barrier in either the entrance or exit channel. The excited-state reaction is exothermic, but there is a barrier in the entrance valley and none in the exit valley. This indicates that the dynamics and accordingly the kinetics of the two reactions can be expected to show significant differences. As a result of the presence of both a well (making possible the formation of long-lived complexes) and a barrier on the PES, the most reliable way to estimate the rate coefficient of the reaction is through reaction dynamics calculations. The PES needed for dynamical studies was developed by Li et al.,⁴⁴ who calculated the potential energy at some 17 000 points and made a spline fit to the calculated points. With this PES, the basic dynamical properties of the reaction were calculated⁴⁵ for the ground vibrational and rotational state of $\text{O}_2(^1\Delta_g)$ using accurate quantum-mechanical methods. Reliable calculation of the thermal rate coefficient from the theoretically derived reaction cross sections, however, was not possible because of the limited range of initial conditions.

Expected Dynamical Behavior Based on the Properties of the Potential Energy Surface. The investigation of the topology of the PES developed by Li et al.⁴⁴ allows one to estimate the qualitative features of the dynamics of the reaction. Sections of the PES are shown in Figure 2, where the potential

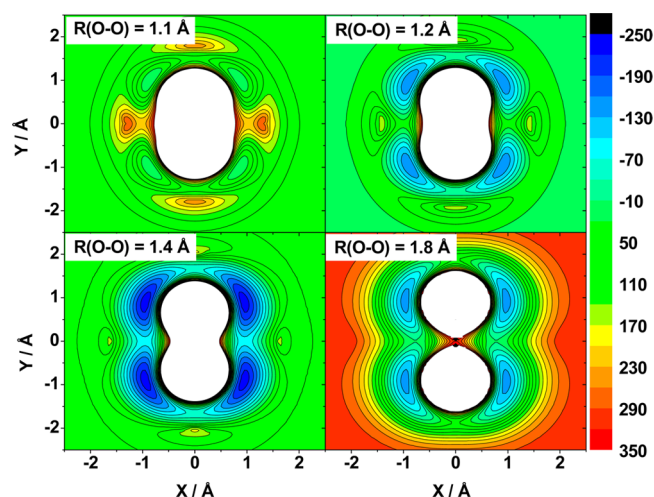


Figure 2. Sections of the potential energy surface for reaction R2 in the H–O–O plane as a function of the location of the H atom with respect to the center of mass of O_2 . O_2 is aligned along the y axis; its bond length is as specified on each plot. The unit of energy is kJ/mol.

energy is plotted as a function of the location of the H atom in the triatomic plane with respect to the center of mass of the O_2 molecule. The O–O distance is set to 1.1 Å, the inner turning point of the ground vibrational state of $\text{O}_2(^1\Delta_g)$; 1.2 Å, the equilibrium bond length of O_2 ; 1.4 Å, the equilibrium O–O distance in electronically excited HO_2 ; or 1.8 Å, which corresponds to a more-or-less separate OH radical and O atom. It should be noted that the PES is cylindrically symmetric around the O–O axis. One can see that a repulsive wall protects the O_2 molecule at the two ends as well from sideways attack. There is a relatively narrow band around both oxygen

atoms where the H atom can approach the molecule. As expected for an exothermic reaction, the barrier is early: the saddle point (at 31.7 kJ/mol) is in the entrance valley but already almost at the same Jacobi angle as that corresponding to the equilibrium geometry of HO₂(A'). The potential well is actually spread to two tori around the O atoms that correspond to the HOO' and HO'O isomers. The electronically excited HO₂ can isomerize without decomposition, as the height of the barrier (located at $R_{OO} = 1.398$ Å) is only 94 kJ/mol from the bottom of the HO₂ potential well, which is well below the H + O₂ asymptote. The location of the entrance barrier in the reactant valley is more clearly visible in Figure 3, which shows

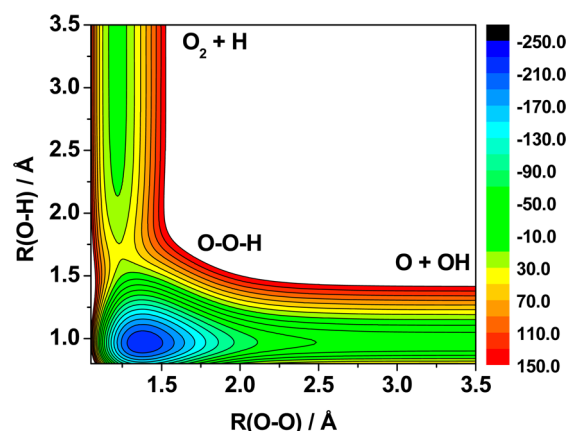


Figure 3. Section of the potential energy surface for reaction R2 as a function of the length of the breaking O–O bond and the forming H–O bond. The H–O–O angle is 112.4°. The unit of energy is kJ/mol.

the PES as a function of the length of the forming and breaking bonds at a fixed H–O–O angle of 112.4° corresponding to the saddle-point geometry (where the O–O and O–H distances are 1.24 and 1.685 Å, respectively). From the features of the PES, one can expect the reactivity of O₂ to depend on its rotational excitation: the cone of acceptance covering the two reactive bands around the O₂ molecule is expanded when the molecule rotates, and the bands sweep almost a complete sphere when O₂ rotates. According to Polanyi's rules,⁴⁶ vibrational excitation would not be efficient to increase the chance for the system to enter the HO₂ well. One can also expect that the stripping-type reactions will involve rotational excitation of the product OH because at the favorable direction of approach the O–O–H arrangement is bent. The distribution of the reaction energy among the product degrees of freedom is not easy to predict because it depends on the time spent in the potential well.

The purpose of the present work is to derive *ab initio* the thermal rate coefficient for reaction R2. To this end, we extend the range of initial conditions, in particular, the number of initial rotational states considered, compared with the earlier dynamics calculations. The purpose is to include in the thermal averaging the high rotational states of O₂, whose populations are significant at flame temperatures. We use the quasiclassical trajectory (QCT) methodology, which—after “calibration” against the existing quantum-dynamical data—not only allows us to get the excitation functions needed for rate coefficient calculations but also provides some insight into the dynamics of reactions on potential surfaces involving a deep potential well with an entrance barrier but no exit barrier.

The rest of the paper is organized as follows: after providing a summary of the methodology, we show the calibration of the QCT method and then present the results on the effect of vibrational and rotational excitation of the reactants on the dynamics of reaction R2, followed by the product state distributions and the thermal rate coefficients. Then we discuss the results on the microscopic dynamics of the reaction.

METHODS

The QCT calculations were performed using an extensively modified version of the VENUS code.⁴⁷ At each collision energy, 2×10^5 trajectories were calculated. For the integration of Hamilton's equation of motion in Cartesian coordinates, the sixth-order Adams–Moulton predictor–corrector algorithm initiated by a fourth-order Runge–Kutta integrator was used. A step size of 0.1 fs was employed for integration. The conservation of the total energy was better than 0.05 kJ/mol. The initial H–O₂ separation was fixed at 9 Å, which guaranteed a negligible initial interaction between H and O₂. On the basis of calculations of the opacity function at several collision energies and O₂ initial quantum states, the maximum impact parameter was set to $b_{\max} = 3.0$ Å. When the impact parameters are Monte Carlo-sampled so that the number of trials in a given impact parameter domain is proportional to the impact parameter, the initial-state-selected reaction cross section is given by

$$\sigma_r(E_{\text{coll}}, \nu, j) = \pi b_{\max}^2 \frac{N_r(E_{\text{coll}}, \nu, j)}{N} \quad (1)$$

where b_{\max} is the maximum impact parameter, N_r is the number of reactive trajectories, N is the total number of trajectories, ν and j denote the initial vibrational and rotational quantum numbers of the reactant molecule, respectively, and E_{coll} is the relative collision energy of the reactants. In the evaluation of trajectories we tested several commonly used techniques, including the following:

1. QCT: all of the reactive trajectories are included in the calculation.
2. QCT-ZP: trajectories producing OH with smaller than 0 vibrational quantum number are discarded without replacement.
3. GW-QCT: trajectories are considered with a Gaussian weight depending on the distance of the final classical action variable of the product molecule from the nearest quantum state.^{48–50} We used the standard value of 0.05 for the width of the Gaussian “window.”

We also recorded the fate of nonreactive trajectories that entered the potential well by recording whether the trajectory entered the region of the configuration space where the energy is below one-half of the dissociation energy of the complex to O + OH, which is 138 kJ/mol below the reactant level. All such trajectories necessarily pass the potential barrier and represent a very conservative estimate of the fraction of trajectories that, after crossing the barrier in the forward direction, will cross it again in the reverse direction.

RESULTS

A. Validation of QCT Calculations. Ma et al.⁴⁵ performed exact quantum scattering (EQ) calculations on the A' PES. They studied the reaction starting from the ground vibrational and rotational state of O₂(¹Δ_g) in the collision energy range of 20–90 kJ/mol. QCT calculations were performed in the same

energy range for the same quantum state to evaluate the performance of the three ways of handling final vibrational states. The results are shown in Figure 4 (Figure S1 in the

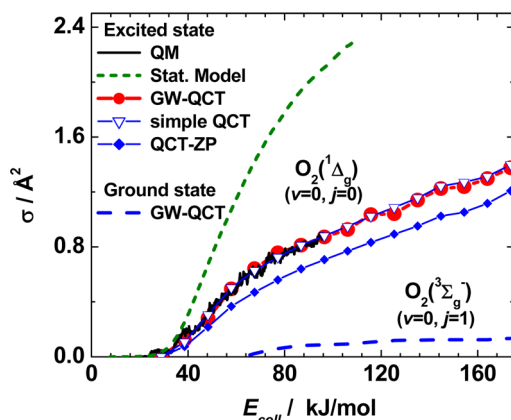


Figure 4. Excitation functions for reactions R1 and R2 calculated with exact and statistical quantum-mechanical methods as well as three versions of the QCT method.

Supporting Information shows the threshold region magnified). The QCT-ZP method considerably underestimates the EQ cross sections. The simple QCT and GW-QCT methods provide very similar cross sections that excellently match those obtained in the EQ calculation (except the sudden rise in the threshold region). We consider this a validation of the simple QCT and GW-QCT methods and assume that they can be reliably used to predict the dynamical details of the reaction outside the region covered by the exact quantum-mechanical method. Hereinafter only the results obtained with the GW-QCT method are presented. It is worth mentioning that the barrier very probably is passed with minimal assistance from vibration (see below). This means that in a system with a barrier before and no barrier after a potential well, the common reasoning that zero-point energy violation in the products is an indicator of nonquantum effects in the reaction loses sense, and omission of trajectories yielding products with less than zero-point energy will lead to misleading results.

B. Integral Cross Sections. The GW-QCT excitation functions for various vib-rotational states of $\text{O}_2(^1\Delta_g)$ are presented in Figure 5 (and in Figure S2 in the Supporting Information, zoomed on the threshold region). The integral cross sections are monotonic functions of the collision energy. The threshold energy is 28.9 kJ/mol at $v = 0$ and $j = 0$. The

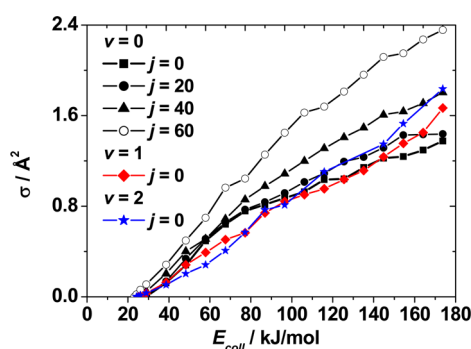


Figure 5. Influence of vibrational and rotational excitation of the reactant $\text{O}_2(^1\Delta_g)$ on the excitation function of reaction R2.

sum of this collision energy and the zero-point energy of the oxygen molecule is 38.1 kJ/mol, 6.4 kJ/mol higher than the entrance channel barrier (31.7 kJ/mol). This indicates that probably only a small fraction of trajectories pass the barrier at the price of zero-point violation, which is in agreement with the early position of the barrier. Investigation of the effect of vibrational excitation on the cross sections further supports the lack of vibrational non-adiabaticity of classical trajectories near the potential barrier. Vibrational excitation of O_2 to $v = 1$ and $v = 2$ reduces the threshold energy by only 3 and 4 kJ/mol, respectively. Furthermore, surprisingly, above the $v = 0$ threshold up to $E_{\text{coll}} = 110$ kJ/mol, the reaction cross sections are smaller when O_2 is vibrationally excited. Rotational excitation of the singlet oxygen molecule up to $j = 20$ does not change the cross sections except at collision energies very close to threshold, reducing the latter by about 1 kJ/mol. At higher excitation the threshold energy is further reduced with increasing j , by about 5 kJ/mol at $j = 40$ and 8 kJ/mol (with respect to the ground rotational state) when $j = 60$, and the cross sections are also larger at individual collision energies. The reduction of the threshold is about 10 times smaller than the rotational energy, indicating that the rotation of O_2 only marginally facilitates the system when crossing the barrier.

The threshold energy from the exact quantum scattering calculations is 21.2 kJ/mol for the reaction of the vib-rotational ground state of $\text{O}_2(^1\Delta_g)$, above which the cross section remains very small until the classical threshold energy, where it starts to increase so that the EQ and QCT excitation functions in fact overlap. Considering this and the lack of zero-point energy violation, one can conclude that the reaction proceeds through tunneling at collision energies between 21 and 31 kJ/mol. Comparison with the excitation function calculated quantum-mechanically for the reaction of H with O_2 in the electronic ground state shows significant enhancement of the reactivity of O_2 toward H atoms by electronic excitation. The threshold energy for the reaction of triplet O_2 is 57.9 kJ/mol, which is much larger than that for O_2 in the excited state. In addition, the magnitudes of the ground-state cross sections are smaller than the excited-state ones by about an order of magnitude at identical collision energies. Both these factors indicate that the reactivity of electronically excited O_2 toward H is much larger than that of triplet molecular oxygen, and one can expect this to be reflected in the rate constants.

C. Differential Cross Sections. Product angular distributions in the center-of-mass frame are shown in Figure 6 (it should be noted that the scale is arbitrary but the magnitude reflects the overall reactivity). Forward–backward symmetry is observed at low collision energies, which is a signature of statistical behavior. At high collision energies, dynamical effects, as expected, are found to be more significant: the forward peak increases, indicating the increasing role of stripping trajectories. Vibrational excitation of O_2 has no significant effect on the angular distribution. Rotational excitation, on the other hand, leads to a reduction in the forward and backward peaks and an increasing role of sideways scattering. In contrast, no well-defined forward and backward peaks can be seen in the angular distributions of nonreactive trajectories that enter the potential well (Figure S3 in the Supporting Information). Signs of preferentially backward scattering are visible but sideways scattering is also remarkable which is in agreement with the features of the PES: the barrier in the entrance channel is at a bent arrangement.

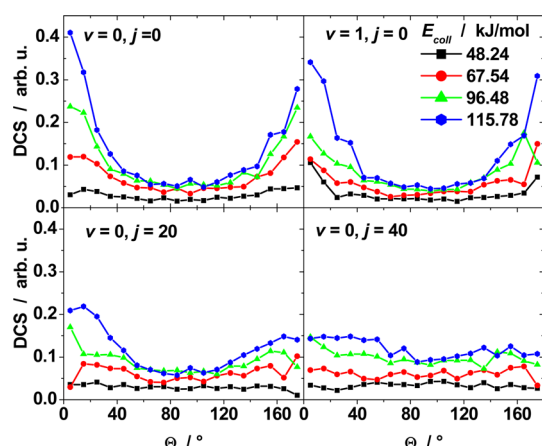


Figure 6. Product angular distributions of reaction R2 starting from various vib-rotational quantum states of $\text{O}_2(^1\Delta_g)$ at several collision energies.

D. Product State Distributions. The products are formed in relatively high rotational states even at low collision energy. Increasing the collision energy induces enhanced product rotational excitation. The vibrationally resolved product rotational distributions are shown in Figure 7. OH is formed

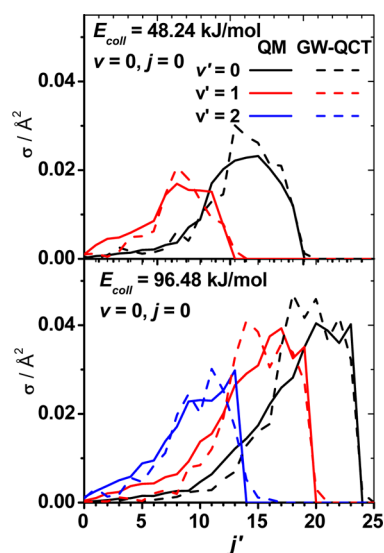


Figure 7. Vibrationally resolved OH rotational distributions in reaction R2 at two collision energies. For comparison, the distributions obtained in exact quantum-mechanical calculations by Ma et al.⁴⁵ are also shown.

either vibrationally or rotationally excited. With increasing collision energy more vibrational channels open, but the shape of the rotational distribution remains almost the same. Remarkably, the distributions provided by the GW-QCT method are in excellent agreement with the exact quantum scattering data. Both (de facto identical) dynamical results deviate from the statistical distribution (as amply discussed in ref 45.) indicating that the complex does not behave statistically. On the other hand, on the basis of the distributions starting from excited rotational states (Figure S4 in the Supporting Information), there seems not to be any preference for conserving rotational energy, which is probably a

consequence of the significant difference in the moments of inertia of the reactant and product diatomics.

E. Thermal Rate Coefficients. The rotational- and vibrational-state-resolved reaction rates were calculated from the excitation functions according to eq 2:

$$k(T, \nu, j) = \left(\frac{8}{\pi\mu} \right)^{1/2} \left(\frac{1}{k_B T} \right)^{3/2} \int_0^\infty \sigma(E_{\text{coll}}, \nu, j) E_{\text{coll}} \exp\left(-\frac{E_{\text{coll}}}{k_B T}\right) dE_{\text{coll}} \quad (2)$$

where $\sigma(E_{\text{coll}}, \nu, j)$ is the state-resolved cross section, E_{coll} is the collision energy, k_B is the Boltzmann constant, and μ is the reduced mass of the collision partners. The initial-state-resolved excitation functions were derived from trajectory calculations at $\nu = 0$ or 1 for all even- j rotational states of O_2 from $j = 0$ to $j = 60$ (as a result of nuclear symmetry, $\text{O}_2(^1\Delta_g)$ has only even quantum states). These very large rotational quantum numbers are needed when thermal averages of j -specific rate coefficients are calculated: because of the large moment of inertia of O_2 , the Boltzmann weight of the highly excited rotational states is not negligible at flame temperatures. For example, above 1000 K the population of rotational levels is significant up to $j = 40$, and it is desirable to include even $j = 60$ in the averaging.

Representative initial- j -resolved rate coefficients are shown in Figure 8. At room temperature, rotational excitation of the

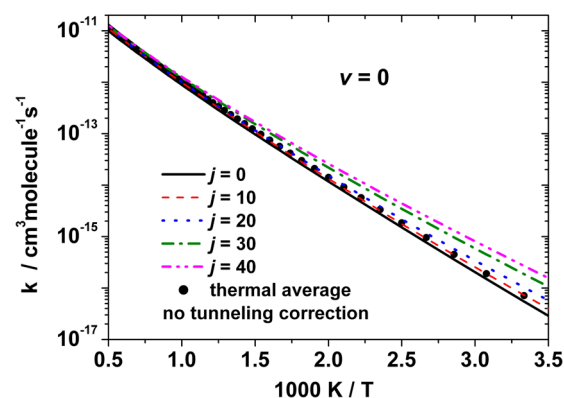


Figure 8. Influence of rotational excitation of the reactant $\text{O}_2(^1\Delta_g)$ on the thermal rate coefficient of reaction R2

oxygen molecule to $j = 40$ increases the rate coefficient by a factor of 5.6, which drops to 1.6 at 1000 K. The j -averaged rate coefficients are close the value of the rate for $j = 10$ at all temperatures and are larger than the $j = 0$ values by a factor of 1.6 at 300 K and 1.2 at 1000 K.

Vibrational excitation of O_2 slightly reduces the reaction cross section and, accordingly, slows down the reaction. This minor hindrance is observable only around 1000 K, where the $\nu = 1$ state of O_2 has appreciable Boltzmann weight.

To obtain more reliable thermal rate coefficients, we introduced a tunneling correction of the vibrationally and rotationally resolved excitation functions as follows: For the reaction of the vib-rotational ground state of $\text{O}_2(^1\Delta_g)$, the EQ excitation function was used at low energies until it first crossed the QCT one. Above that energy, the QCT cross section was used in the rate coefficient calculation. For the description of tunneling at higher j and ν , the same fragment of the quantum scattering excitation function was applied in a similar way to

modify the classical excitation function (i.e., the same tunneling behavior was assumed for each quantum state). Specifically, for the vib-rotational ground-state reaction, the EQ excitation function first crosses the QCT one at $E_{\text{coll}} = 32.8$ kJ/mol, $\sigma = 0.0335$ Å². For excited vib-rotational states of O₂(¹Δ_g), the section of the EQ excitation function between $E_{\text{coll}} = 22$ kJ/mol (the EQ threshold) and 32.8 kJ/mol was shifted along the E_{coll} axis until its right-hand end matched the $\sigma = 0.0335$ Å² value of the relevant QCT excitation function (Figure 9). Below that

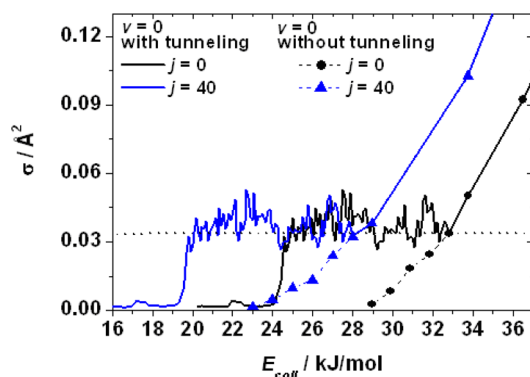


Figure 9. Combined (QM + QCT) excitation functions used for tunneling correction at different rotational states of O₂(¹Δ_g) in the threshold region obtained by merging the classical and QM curves at cross section $\sigma = 0.0335$ Å² (indicated by a dotted straight line).

energy the QCT cross section was replaced by the EQ one. This correction is based on the quantum-mechanical reactive flux, so below $\sigma = 0.0335$ Å² it covers all of the quantum effects, including not only underbarrier tunneling but also quantum effects corresponding to barrier recrossing. It should be noted that these contributions cannot be separated.

The tunneling-corrected thermal reaction rate coefficient averaged over the Boltzmann distribution of initial rotational and vibrational states is shown in Figure 10 together with the

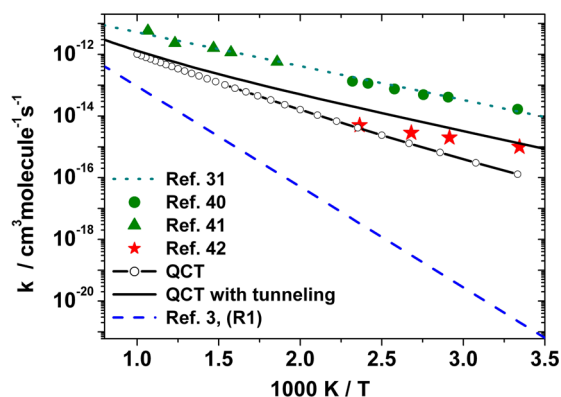


Figure 10. Comparison of the experimental and calculated thermal rate coefficients for reaction R2. The blue dashed line shows the data recommended by Baulch et al.³ for reaction R1.

experimental data (Figure S5 in the Supporting Information shows the j -dependent tunneling-corrected rate coefficients). The rate coefficient including the tunneling correction as described above is 1.34×10^{-15} cm³ molecule⁻¹ s⁻¹ at 300 K, 1.31×10^{-12} cm³ molecule⁻¹ s⁻¹ at 1000 K, and 1.18×10^{-11} cm³ molecule⁻¹ s⁻¹ at 2000 K. (The enhancement of the thermally averaged rate coefficient due to tunneling is a factor

of 9.3 at 300 K and 1.3 at 1000 K.) The calculated values are closer to the measured data of Hack and Kurzke⁴² than to those of the experiments where reaction and electronic quenching were not separated. The deviation from the Hack and Kurzke rate coefficients is only a factor of 1.2 at the lowest and 3 at the highest measured temperature. The average Arrhenius activation energy (Table 1) for the rate constants thermally averaged over the initial states is 24.4 kJ/mol, which is larger than that proposed by Hack and Kurzke but close to that derived by Popov³¹ from the measurements including quenching and chemical reaction.

Comparison of the rate coefficients for the reactions of H atoms with O₂(¹Δ_g) and with O₂(³Σ_g⁺) shows that electronic excitation enhances the reactivity of O₂ toward H. At low flame temperatures, the rate coefficient for the reaction with excited O₂(¹Δ_g) is 4 or 5 orders of magnitude higher than that with O₂(³Σ_g⁺), while at 1000 and 2000 K the differences are by factors of about 13 and 3, respectively. This is in good agreement with the observation that the presence of O₂(¹Δ_g) speeds up flame propagation. If one accepts that the rate coefficients measured by Cupitt et al.⁴⁰ and by Basevich and Vedenev⁴¹ include both reactive and nonreactive quenching, then from the ratio of these experimental rate constants (interpolated using the formula derived by Popov) to those derived from the QCT calculations one can estimate that nonreactive quenching is 3–12 times faster than the chemical reaction.

It is interesting to note that as long as the conditions in flames ensure thermal equilibrium between ground-state and singlet molecular oxygen, the populations of the latter are about 0.1%, 0.6%, and 1.9% at 1500, 2000, and 2500 K, respectively. As long as these equilibrium populations hold in shock tubes, where the experimental rate coefficients for reaction R1 were obtained, the measured data contain contributions of 0.5%, 1.9%, and 4.7% from reaction R2, respectively. These are much smaller than the experimental error bars, so there is no need to make a correction. It can also be noted that although at high temperatures the contribution of reaction R2 to the thermal average rate of reactions R1 and R2 increases quickly (it would reach 30% at 5000 K), it will never be larger than that of reaction R1 because at high temperatures reaction R1 is also very fast.

DISCUSSION

The potential energy surface of reaction R2 has a unique feature: there is a potential barrier in the entrance channel, which is followed by a deep potential well on the way to products. The dynamics of this type of reaction has not been widely studied. A number of interesting questions arise for this combination of PES features, including the following: (1) Do Polanyi's rules⁴⁶ hold for such reactions? (2) How does the formation of the complex after passing the entrance barrier (with energies significantly above product channel energy) influence the dynamics of the reaction? (3) Is the behavior of the complex formed statistical or nonstatistical, including (4) does the state distribution of nonreactive trajectories that entered the complex region show signs of complex formation and (5) is the barrier recrossed by a significant fraction of the trajectories that pass it in the forward direction?

Concerning Polanyi's rules, the basic piece of information is that the potential barrier is in the reactant valley. From this one can expect that vibration is not the preferred degree of freedom for promoting the reaction. In accord with this expectation, in

the dynamical studies the threshold energy for the reaction of singlet O_2 was found to be essentially the same with or without vibrational excitation of the reactant. At energies above the threshold, the reactive cross sections for $\nu = 1$ are somewhat smaller than those at $\nu = 0$ at identical collision energies. This shows that in inducing reaction, vibrational energy is much less effective than translation. If the reaction cross section is plotted against the sum of the vibrational and translational energy, the excitation function for $\nu = 1$ is shifted to higher energies with respect to that corresponding to $\nu = 0$ by the amount of the energy in vibration (17.7 kJ/mol for $\nu = 1$ with respect to zero-point energy). All of these facts indicate that the dynamics of the reaction follows Polanyi's rules. However, one has to keep in mind that passing the barrier does not necessarily mean that the trajectory will be reactive but guarantees only that the system will enter the potential well. The number and behavior of possible trajectories that enter the well but cross again and depart as nonreactive is a key factor in characterizing the dynamics of this system.

When one monitors the potential energy of individual trajectories, they turn out to pass the barrier region with a potential energy hardly exceeding the saddle-point energy (generally by not more than a few kJ/mol) when the O_2 initially is in the vibrational ground state. The spread is larger for $\nu = 1$ or 2, but this can be understood to be a consequence of the larger amplitude of the oscillation around the minimum-energy path. This also suggests that for vibrationally ground-state oxygen, the system does not need to borrow energy from vibration to pass the barrier, even though the latter is at the early part of the curvature of the minimum-energy path. From this it follows that for this reaction, zero-point violation at the barrier crossing as a classical artifact is of limited importance and would probably not lead to a significant reduction of the threshold energy. This means that the reason why the QCT-ZP reaction cross sections are smaller than the simple QCT (or GW-QCT) ones is not the ZPE violation at the barrier crossing. Instead, many trajectories, after entering the HO_2 potential well without vibrational energy leakage, undergo some vibrational energy redistribution and emerge on the product side as OH with less than zero-point energy.

To understand the details of the dynamics, we monitored trajectories that enter the deep part of the potential well (i.e., ones in which H and O_2 form a complex). To this end, we recorded the trajectories that access the region of the configuration space where the potential energy is one-half of the dissociation energy of the complex to $\text{O} + \text{OH}$ (138 kJ/mol below the reactant level). The number of collisions getting into this region provides a very conservative estimate of the rate of complex formation. This is in fact a capture model (the classical analogue of the quantum capture theory used by Ma et al.). What is more in our QCT calculations is that in our model, dynamics is partly introduced by following the trajectories even after capture. This enables us to tell apart reactive and nonreactive captured trajectories. The cross section for complex formation (including both reactive and nonreactive collisions) is plotted against the collision energy in Figure 11 (and in Figure S6 in the Supporting Information, zoomed on the threshold region). The threshold for entering the potential well is the same for reactive and nonreactive collisions, and the ratio of reactive cross section to the complex-forming nonreactive cross section remains constant as the collision energy increases. About 4 times more trajectories leave the complex in the reactant direction than toward products. This means that about

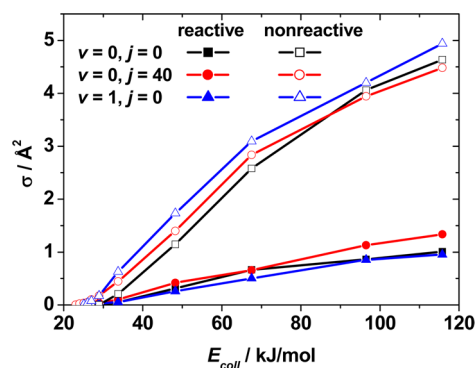


Figure 11. Cross sections characterizing complex formation by H and $\text{O}_2(^1\Delta_g)$. See the text for details.

80% of the trajectories cross the barrier at least twice, once from the reactant side and once in the opposite direction (the chance of passing it more than twice is negligible). This holds not only at high collision energies but also in the threshold region. On this basis, one can conclude that one of the basic assumptions of transition state theory, the existence of a “point of no return”, is not fulfilled for this reaction: one cannot find a dividing surface in the barrier region that satisfies the condition that no trajectory crosses it more than once. The observations made using quasiclassical trajectories are in good agreement with the earlier quantum-statistical^{51,52} calculations,^{44,45} which were found to overestimate the reaction cross sections by a factor of 2.3. (A possible explanation for the difference in the numerical values of the factors is that the two models use different definitions for capture.)

Further information can be gained from the lifetime distribution of the collision complexes. An exponential lifetime distribution characterizes complexes that decay completely randomly,⁵³ in other words, the phase space points are uniformly accessible. This is one of the conditions for the applicability of statistical theories of reaction rates to the decomposition of the complex. The lifetime of the collision complex was calculated as a classical analogue to Smith's collision lifetime matrix:⁵⁴ the lifetime is the delay caused by the interaction as compared to an inelastic hard-sphere collision. The lifetime then is obtained from the total duration of the collision by subtracting the time of inbound flight from the initial center-of-mass separation to 3 Å and the analogous outbound flight time.

The lifetime distributions of the reactive and complex-forming nonreactive trajectories for various sets of initial conditions are shown in Figure 12. In the reaction of $\text{O}_2(^1\Delta_g)$ in its vib-rotational ground state, at low collision energies the contribution of prompt reactive trajectories is small. This means that if the barrier is passed with a small excess translational energy, a significant time (about 0.5 ps) is needed for the system to find its way out in the product direction. Below $E_{\text{coll}} = 48.24$ kJ/mol, in the majority of reactive collisions a relatively long-lived complex (lifetime > 0.5 ps) is formed. The distribution of lifetimes longer than 0.5 ps is close to exponential up to about $E_{\text{coll}} = 67.5$ kJ/mol. This observation is in line with the forward–backward symmetry of the product angular distributions shown in Figure 6 for low collision energies. At higher collision energies, instantaneous reactive collisions dominate. This means that at higher impact energy the trajectories do not spread within the region of configuration space corresponding to the potential well; instead, they more-

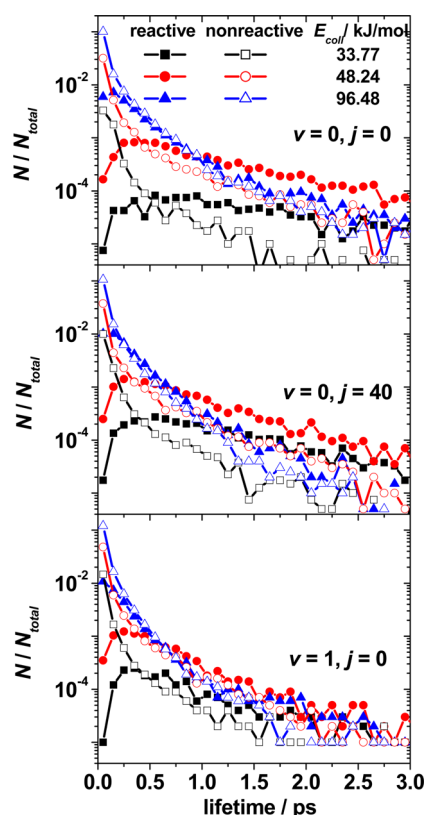


Figure 12. Lifetime distributions of complex-forming reactive (closed symbols) and nonreactive (open symbols) collisions in reaction R2 for various collision energies and reactant quantum states.

or-less keep their initial momentum and get out of the well relatively quickly. The decay rate constant, given by inverse of the approximate lifetime of the long-lived reactive complex, is in the range of 7×10^{11} to $2 \times 10^{12} \text{ s}^{-1}$ and increases linearly with the collision energy. This is in agreement with the nearly linear increase in the excitation function.

The majority of complex-forming collisions are nonreactive. The lifetime distribution of such collision complexes peaks at the first calculated time bin, and only a small fraction of such complexes survive longer than 0.5 ps. Animation of individual trajectories showed that such a short time is enough for the O–H bond to make several oscillations after the system enters the well across the barrier and before it leaves the same way. The decay rate coefficient for the complexes living longer than 0.5 ps is approximately a factor of 3 larger than that of long-lived reactive ones at low collision energies; the factor decreases to 1 when E_{coll} is about 100 kJ/mol. As the energy needed for the complexes to return to reactants is much higher than that for the complexes to decompose to products, this behavior is again an indication that the HO_2 complex does not behave statistically. Another indication comes from the comparison of complex lifetimes when approximately the same total amount of energy is provided in different degrees of freedom (Figure 13): $v = 0, j = 0, E_{\text{coll}} = 67.5 \text{ kJ/mol}$; $v = 1, j = 0, E_{\text{coll}} = 49.2 \text{ kJ/mol}$; or $v = 0, j = 40, E_{\text{coll}} = 49.2 \text{ kJ/mol}$. In addition to the large variation in the magnitude of the reactivity, the decay rate of long-lived complexes is smaller when the initial energy comes in the form of vibration and especially of rotation.

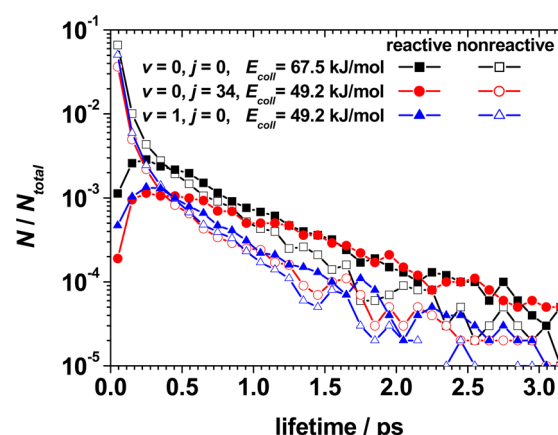


Figure 13. Lifetime distribution of complex-forming reactive (solid symbols) and nonreactive (open symbols) collisions in reaction R2 when the same total amount of energy is provided in different degrees of freedom.

CONCLUSIONS

The present QCT calculations on the $\text{H} + \text{O}_2(^1\Delta_g)$ reaction have extended the range of initial conditions in the previous quantum scattering calculations to vibrationally and rotationally excited reactants. Both the simple QCT method and the GW-QCT method (see Methods) yield excellent agreement with the exact quantum scattering calculations⁴⁵ for the excitation function of the reaction of vib-rotationally ground state $\text{O}_2(^1\Delta_g)$. Moreover, the product vibrational and rotational distributions also overlap almost perfectly with the exact quantum results. The cross sections proved to be hardly sensitive to vibrational excitation of the oxygen molecule. Rotational excitation is favorable for the reaction, but only a small fraction of the rotational energy is utilized.

The unique nature of the potential energy surface of the reaction, namely, a small barrier in the entrance valley followed by a deep potential well, makes the dynamics curious. The expectation based on Polanyi's rule that vibrational energy is less effective than translational energy at inducing reaction is fulfilled: vibrational excitation does not reduce the threshold energy. Moreover, vibrational excitation of O_2 not only is not favorable for inducing reaction but even has an opposite effect: (i) above threshold it slightly reduces the cross sections at the same translational energy even though much more energy is available for the reactants to cross the barrier, and (ii) the cross sections significantly decrease when the ratio of the vibrational energy to the translational energy is increased at the same total energy.

After the barrier is crossed, for reaction to happen the system needs to pass the potential well. Out of the collisions entering the complex region, 80% return across the barrier and reproduce the reactants, which means that transition state theory cannot be expected to realistically predict the rate of the reaction. The collision lifetime distributions show that reactive trajectories emerge from the potential well with a delay in contrast to the mostly prompt nonreactive complex-forming ones. The lifetime distribution of long-lived HO_2 complexes is close to exponential at low energies, but the decay rate back to the energetically less favorable reactants through the higher barrier is larger than that for decomposition into products. The complex lifetime varies when the initial energy is provided in different degrees of freedom, indicating ineffective energy

redistribution. From this one can conclude that statistical theory cannot properly describe the behavior of relatively long lived complexes either. Interestingly, at low collision energy the product angular distributions exhibit forward–backward symmetry because most of the reactive events involve a long-lived complex; in this reaction, however, this does not mean that the complexes behave statistically.

The thermal rate coefficient calculated from cross sections (taking tunneling into account) agrees well with the measured data of Hack and Kurzke⁴² and can be described by the extended Arrhenius form $k_2 = 5.81 \times 10^{-16} T^{1.45} \exp(-2270/T)$ cm³ molecule⁻¹ s⁻¹ over the temperature range of 200–3000 K. Taking into account the fact that the experiments of Cupitt et al.⁴⁰ and Basevich and Vedenev⁴¹ determined the rate of both the reactive and nonreactive quenching of O₂(¹Δ_g) and obtained almost an order of magnitude larger rate coefficients, one can estimate that the nonreactive quenching is between 12 times (at 300 K) and about 3 times (at 1000 K) faster than reaction R2.

Comparison of the reactivities of H atoms with triplet molecular oxygen and O₂(¹Δ_g) shows that electronic excitation increases the rate coefficient by 4 or 5 orders of magnitude at low temperatures and by a factor of about 10 at high flame temperatures. This means that the presence of singlet molecular oxygen in flames facilitates combustion by increasing the chain-branching step, in agreement with numerous simulations. It should be noted that in combustion modeling, the rate coefficient derived from the measurements of Cupitt et al.⁴⁰ and Basevich and Vedenev⁴¹ is in general use. The current calculations show that these rate coefficients are too large by about an order of magnitude, in agreement with the work of Hack and Kurzke.⁴² This means that the simulations applying the rate coefficients including both reaction and electronic quenching in lieu of reaction R2 may overestimate the effect of singlet molecular oxygen on the rate of combustion.

■ ASSOCIATED CONTENT

■ Supporting Information

Complete ref 3 and figures showing product angular and vibrational distributions, rate coefficients for reactions starting from various rotational states of singlet O₂, and versions of Figures 4, 5 and 11 zoomed on the threshold region. This material is available free of charge via the Internet at <http://pubs.acs.org>.

■ AUTHOR INFORMATION

Corresponding Author

*E-mail: lendvay.gyorgy@ttk.mta.hu. Phone: +36-1-382-6508.

Notes

The authors declare no competing financial interest.

■ ACKNOWLEDGMENTS

We are grateful to Professors Hua Guo and Daiqin Xie for providing us with the PES code and the quantum dynamical data. This work was supported in part by the Hungarian Scientific Research Fund (Grants OTKA T77938 and K108966) and by the National Development Agency (Grants KTIA_AIK_12-1-2012-0014 and TÁMOP-4.2.2.A-11/1/KONV-2012-0064).

■ REFERENCES

- (1) Miller, J. A.; Kee, R. J.; Westbrook, C. K. Chemical Kinetics and Combustion Modeling. *Annu. Rev. Phys. Chem.* **1990**, *41*, 345–387.
- (2) Miller, J. A.; Pilling, M. J.; Troe, J. Unraveling Combustion Mechanisms through a Quantitative Understanding of Elementary Reactions. *Proc. Combust. Inst.* **2005**, *30*, 43–88.
- (3) Baulch, D. L.; Bowman, C. T.; Cobos, C. J.; Cox, R. A.; Just, Th.; Kerr, J. A.; Pilling, M. J.; Stocker, D.; Troe, J.; Tsang, W.; et al. Evaluated Kinetic Data for Combustion Modeling: Supplement II. *J. Phys. Chem. Ref. Data* **2005**, *34*, 757–1397.
- (4) Pirraglia, A. N.; Michael, J. V.; Sutherland, J. W.; Klemm, R. B. A Flash Photolysis–Shock Tube Kinetic Study of the Hydrogen Atom Reaction with Oxygen: $H + O_2 \rightleftharpoons OH + O$ ($962\text{ K} \leq T \leq 1705\text{ K}$) and $H + O_2 + Ar \rightarrow HO_2 + Ar$ ($746\text{ K} \leq T \leq 987\text{ K}$). *J. Phys. Chem.* **1989**, *93*, 282–291.
- (5) Frank, P.; Just, Th. High Temperature Reaction Rate for $H + O_2 = OH + O$ and $OH + H_2 = H_2O + H$. *Ber. Bunsen-Ges. Phys. Chem.* **1985**, *89*, 181–187.
- (6) Masten, D. A.; Hanson, R. K.; Bowman, C. T. Shock Tube Study of the Reaction $H + O_2 \rightarrow OH + O$ Using OH Laser Absorption. *J. Phys. Chem.* **1990**, *94*, 7119–7128.
- (7) Yuan, T.; Wang, C.; Yu, C.-L.; Frenklach, M.; Rabinowitz, M. J. Determination of the Rate Coefficient for the Reaction $H + O_2 \rightarrow OH + O$ by a Shock Tube/Laser Absorption/Detailed Modeling Study. *J. Phys. Chem.* **1991**, *95*, 1258–1265.
- (8) Shin, K. S.; Michael, J. V. Rate Constants for the Reactions $H + O_2 \rightarrow OH + O$ and $D + O_2 \rightarrow OD + O$ over the Temperature Range 1085–2278 K by the Laser Photolysis–Shock Tube Technique. *J. Chem. Phys.* **1991**, *95*, 262–273.
- (9) Du, H.; Hessler, J. P. Rate Coefficient for the Reaction $H + O_2 \rightarrow OH + O$: Results at High Temperatures, 2000 to 5300 K. *J. Chem. Phys.* **1992**, *96*, 1077–1092.
- (10) Hwang, S. M.; Ryu, S.-O.; Witt, K. J.; Rabinowitz, M. J. High Temperature Rate Coefficient Measurements of $H + O_2$ Chain-Branching and Chain-Terminating Reaction. *Chem. Phys. Lett.* **2005**, *408*, 107–111.
- (11) Hong, Z.; Davidson, D. F.; Barbour, E. A.; Hanson, R. K. A New Shock Tube Study of the $H + O_2 \rightarrow OH + O$ Reaction Rate Using Tunable Diode Laser Absorption of H₂O Near 2.5 μm. *Proc. Combust. Inst.* **2010**, *33*, 309–316.
- (12) Varandas, A. J. C.; Brandao, J.; Quintales, L. A. M. A Realistic Hydroperoxo (HO₂(X²A'')) Potential Energy Surface from the Double Many-Body Expansion Method. *J. Phys. Chem.* **1988**, *92*, 3732–3742.
- (13) Quintales, L. A. M.; Varandas, A. J. C.; Alvarino, J. M. Quasi-Classical Trajectory Calculations of Thermal Rate Coefficient for the $O + OH \rightarrow O_2 + H$ Reaction on Realistic Double Many-Body Expansion Potential Energy Surfaces for Ground-State HO₂. *J. Phys. Chem.* **1988**, *92*, 4552–4555.
- (14) Varandas, A. J. C. Excitation Function for $H + O_2$ Reaction: A Study of Zero-Point Energy Effects and Rotational Distributions in Trajectory Calculations. *J. Chem. Phys.* **1993**, *99*, 1076–1085.
- (15) Xie, D.; Xu, C.; Ho, T.-S.; Rabitz, H.; Lendvay, G.; Lin, S. Y.; Guo, H. Global Analytical Potential Energy Surfaces for HO₂(X²A'')) Based on High Level Ab Initio Calculations. *J. Chem. Phys.* **2007**, *126*, No. 074315.
- (16) Harding, L. B.; Maergoiz, A. I.; Troe, J.; Ushakov, V. G. Statistical Rate Theory for the $HO + O \rightarrow HO_2 \rightarrow H + O_2$ Reaction System: SACM/CT Calculations between 0 and 5000 K. *J. Chem. Phys.* **2000**, *113*, 11019–11034.
- (17) Troe, J.; Ushakov, V. G. Theoretical Studies of the $HO + O \rightarrow HO_2 \rightarrow H + O_2$ Reaction. II. Classical Trajectory Calculations on an Ab Initio Potential for Temperatures between 300 and 5000 K. *J. Chem. Phys.* **2001**, *115*, 3621–3628.
- (18) Harding, L. B.; Troe, J.; Ushakov, V. G. Classical Trajectory Calculations of the High Pressure Limiting Rate Constants and of Specific Rate Constants for the Reaction $H + O_2 \rightarrow HO_2$: Dynamic Isotope Effects between Tritium + O₂ and Muonium + O₂. *Phys. Chem. Chem. Phys.* **1999**, *2*, 631–642.

- (19) Michael, J. V.; Sutherland, J. W.; Harding, L. B.; Wagner, A. F. Initiation in H_2/O_2 : Rate Constants for $\text{H}_2 + \text{O}_2 \rightarrow \text{H} + \text{HO}_2$ at High Temperature. *Proc. Combust. Inst.* **2000**, *28*, 1471–1478.
- (20) Troe, J. The Struggle for Precise Rate Constants in Gas Phase Reaction Kinetics: The Reaction $\text{H} + \text{O}_2 \rightarrow \text{HO} + \text{O}$. *Z. Phys. Chem.* **2003**, *217*, 1303–1317.
- (21) Lendvay, G.; Xie, D.; Guo, H. Mechanistic Insights into the $\text{H} + \text{O}_2 \rightarrow \text{OH} + \text{O}$ Reaction from Quasi-Classical Trajectory Studies on a New Ab Initio Potential Energy Surface. *Chem. Phys.* **2008**, *349*, 181–187.
- (22) Sun, Z.; Zhang, D. H.; Xu, C.; Zhou, S.; Xie, D.; Lendvay, G.; Lee, S.-Y.; Lin, S. Y.; Guo, H. State-to-State Dynamics of $\text{H} + \text{O}_2$ Reaction, Evidence for Nonstatistical Behavior. *J. Am. Chem. Soc.* **2008**, *130*, 14962–14963.
- (23) Lin, S. Y.; Xie, D.; Guo, H. Revelation of Non-Statistical Behavior in HO_2 Vibration by a New Ab Initio Potential Energy Surface. *J. Chem. Phys.* **2006**, *125*, No. 091103.
- (24) Guo, H. Quantum Dynamics of Complex-Forming Reactions. *Int. Rev. Phys. Chem.* **2012**, *31*, 1–68.
- (25) Lin, S. Y.; Guo, H.; Honvault, P.; Xie, D. Quantum Dynamics of the $\text{H} + \text{O}_2 \rightarrow \text{O} + \text{OH}$ Reaction on an Accurate Ab Initio Potential Energy Surface. *J. Phys. Chem. B* **2006**, *110*, 23641–23643.
- (26) Honvault, P.; Lin, S. Y.; Xie, D.; Guo, H. Differential and Integral Cross Sections for the $\text{H} + \text{O}_2 \rightarrow \text{HO} + \text{O}$ Combustion Reaction. *J. Phys. Chem. A* **2007**, *111*, 5349–5352.
- (27) Lin, S. Y.; Sun, Z.; Guo, H.; Zhang, D. H.; Honvault, P.; Xie, D.; Lee, S.-Y. Fully Coriolis Coupled Quantum Studies of the $\text{H} + \text{O}_2(v_i = 0-2, j_i = 0, 1) \rightarrow \text{OH} + \text{O}$ Reaction on an Accurate Potential Energy Surface: Integral Cross Sections and Rate Constants. *J. Phys. Chem. A* **2008**, *112*, 602–611.
- (28) Basevich, V. Ya.; Kogaro, S. M. O Mekhanizme Vliyaniya Produktov Tleyushchego Razryada na Skorost' Vodorodno–Kislородnikh Plamen v Usloviyah Poluostrava Vosplamneniya [On the Mechanism of the Products of Glow Discharge on the Rate of Hydrogen–Oxygen Flames under the Conditions of the Ignition Peninsula]. *Kinet. Katal.* **1966**, *7*, 393–401.
- (29) Huber, K. P.; Herzberg, G. *Molecular Spectra and Molecular Structure IV: Constants of Diatomic Molecules*; Van Nostrand Reinhold: New York, 1979.
- (30) Sandor, B. J.; Clancy, R. T.; Rusch, D. W.; Randall, C. E.; Eckman, R. S.; Siskind, D. S.; Muhleman, D. O. Microwave Observations and Modeling of $\text{O}_2(^1\Delta_g)$ and O_3 Diurnal Variation in the Mesosphere. *J. Geophys. Res.: Atmos.* **1997**, *102*, 9013–9028.
- (31) Popov, N. A. The Effect of Nonequilibrium Excitation on the Ignition of Hydrogen–Oxygen Mixtures. *High Temp.* **2007**, *45*, 261–279.
- (32) Bourig, A.; Thévenin, D.; Martin, J.-P.; Janiga, G.; Zähringer, K. Numerical Modeling of H_2-O_2 Flames Involving Electronically-Excited Species ($\text{a}^1\Delta_g$), $\text{O}(^1\text{D})$ and $\text{OH}(^2\Sigma^+)$. *Proc. Combust. Inst.* **2000**, *28*, 1471–1478.
- (33) Ombrello, T.; Wona, S. H.; Jua, Y. Flame Propagation Enhancement by Plasma Excitation of Oxygen. Part II: Effects of $\text{O}_2(\text{a}^1\Delta_g)$. *Combust. Flame* **2010**, *157*, 1906–1915.
- (34) Basevich, V. Ya.; Belyaev, A. A. Raschet Uvelicheniya Skorosti Vodorodno–Kislородnogo Plameni Pri Dobavki Singletnogo Oksigena [Calculation of the Enhancement of the Rate of Hydrogen–Oxygen Flames by Addition of Singlet Oxygen]. *Khim. Fiz.* **1989**, *8*, 1124–1129.
- (35) Chukalovsky, A. A.; Rakhimova, T. V.; Klopovsky, K. S.; Popov, N. A.; Mankelevich, Yu. A.; Proshina, O. V. Specific Features of the Kinetics of $\text{H}_2-\text{O}_2-\text{O}_2(\text{a}^1\Delta_g)$ Mixtures: I. Formation and Quenching of Electronically and Vibrationally Excited $\text{HO}_2^*(\text{A}')$ Molecules in $\text{H}_2-\text{O}_2-\text{O}_2(\text{a}^1\Delta_g)$ Mixtures at a Temperature of 300 K. *Plasma Phys. Rep.* **2014**, *40*, 34–51.
- (36) Smirnov, V. V.; Stelmakh, O. M.; Fabelinsky, V. I.; Kzolov, D. N.; Starik, A. M.; Titova, N. S. On the Influence of Electronically Excited Oxygen Molecules on Combustion of Hydrogen–Oxygen Mixture. *J. Phys. D: Appl. Phys.* **2008**, *41*, No. 192001.
- (37) Brown, R. L. An Upper Limit for the Rate of Destruction of $\text{O}_2(^1\Delta_g)$ by Atomic Hydrogen. *J. Geophys. Res.: Space Phys.* **1970**, *75*, 3935–3936.
- (38) Westenberg, A. A.; Roscoe, J. M.; DeHaas, N. Rate Measurement on $\text{N} + \text{O}_2(\text{a}^1\Delta_g) \rightarrow \text{NO} + \text{O}$ and $\text{H} + \text{O}_2(\text{a}^1\Delta_g) \rightarrow \text{OH} + \text{O}$. *Chem. Phys. Lett.* **1970**, *7*, 597–599.
- (39) Schmidt, C.; Schiff, H. I. Reactions of Singlet Oxygen with Atomic Nitrogen and Hydrogen. *Chem. Phys. Lett.* **1973**, *23*, 339–342.
- (40) Cupitt, L. T.; Takacs, G. A.; Glass, G. P. Reaction of Hydrogen Atoms and $\text{O}_2(^1\Delta_g)$. *Int. J. Chem. Kinet.* **1982**, *14*, 487–497.
- (41) Basevich, V. Ya.; Vedeneev, V. I. Konstanta Skorost'i Reakcii $\text{H} + \text{O}_2(^1\Delta) = \text{OH} + \text{O}$ [The Rate Constant of the $\text{H} + \text{O}_2(^1\Delta) = \text{OH} + \text{O}$ Reaction]. *Khim. Fiz.* **1985**, *4*, 1102–1108.
- (42) Hack, W.; Kurzke, H. Kinetic Study of the Elementary Chemical Reaction $\text{H}(\text{S}_{1/2}) + \text{O}_2(^1\Delta_g) \rightarrow \text{OH}(^2\Pi) + \text{O}(^3\text{P})$ in the Gas Phase. *J. Phys. Chem.* **1986**, *90*, 1900–1906.
- (43) Starik, A. M.; Titova, N. S. Possibility of Initiation of Combustion of CH_4-O_2 (Air) Mixtures with Laser-Induced Excitation of O_2 Molecules. *Combust., Explos. Shock Waves* **2004**, *40*, 499–510.
- (44) Li, A.; Xie, D.; Dawes, R.; Jasper, A. W.; Ma, J.; Guo, H. Global Potential Energy Surface, Vibrational Spectrum, and Reaction Dynamics of the First Excited ($\text{A}^2\text{A}'$) State of HO_2 . *J. Chem. Phys.* **2010**, *133*, No. 144306.
- (45) Ma, J.; Guo, H.; Xie, C.; Li, A.; Xie, D. State-to-State Quantum Dynamics of the $\text{H}(^2\text{S}) + \text{O}_2(\text{a}^1\Delta_g) \rightarrow \text{O}(^3\text{P}) + \text{OH}(^2\Pi)$ Reaction on the First Excited State of $\text{HO}_2(\text{A}^2\text{A}')$. *Phys. Chem. Chem. Phys.* **2011**, *13*, 8407–8413.
- (46) Polanyi, J. C. Concepts in Reaction Dynamics. *Acc. Chem. Res.* **1972**, *5*, 161–168.
- (47) Hase, W. L.; Duchovic, R. J.; Lu, D.-H.; Swamy, K. N.; Vande Linde, S. R.; Wolf, R. J. *VENUS: A General Chemical Dynamics Computer Program*; Wayne State University: Detroit, MI, 1988.
- (48) Banares, L.; Aoiz, F. J.; Honvault, P.; Bussery-Honvault, B.; Launay, J.-M. Quantum Mechanical and Quasi-classical Trajectory Study of the $\text{C}(^1\text{D}) + \text{H}_2$ Reaction Dynamics. *J. Chem. Phys.* **2003**, *118*, 565–568.
- (49) Bonnet, L.; Rayez, J.-C. Quasiclassical Trajectory Method for Molecular Scattering Processes: Necessity of a Weighted Binning Approach. *Chem. Phys. Lett.* **1997**, *277*, 183–190.
- (50) Bonnet, L.; Rayez, J.-C. Gaussian Weighting in the Quasiclassical Trajectory Method. *Chem. Phys. Lett.* **2004**, *397*, 106–109.
- (51) Rackham, E. J.; Huarte-Larranaga, F.; Manolopoulos, D. E. Coupled-Channel Statistical Theory of the $\text{N}(^2\text{D}) + \text{H}_2$ and $\text{O}(^1\text{D}) + \text{H}_2$ Insertion Reactions. *Chem. Phys. Lett.* **2001**, *343*, 356–364.
- (52) Rackham, E. J.; Gonzalez-Lezana, T.; Manolopoulos, D. E. A Rigorous Test of the Statistical Model for Atom–Diatom Insertion Reactions. *J. Chem. Phys.* **2003**, *119*, 12895–12907.
- (53) Forst, W. *Theory of Unimolecular Reactions*; Academic Press: New York, 1973.
- (54) Smith, F. T. Lifetime Matrix in Collision Theory. *Phys. Rev.* **1960**, *118*, 349–356.

■ NOTE ADDED AFTER ASAP PUBLICATION

This paper was published ASAP on February 23, 2015. The exponent in the formula giving the temperature dependence of the calculated rate coefficient had been mistyped. The corrected version was reposted on April 22, 2015.